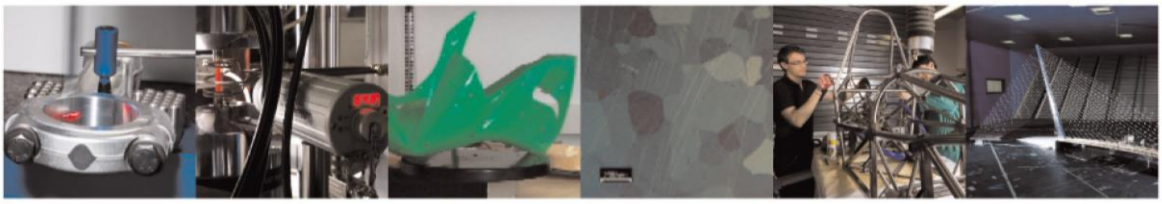

A phase I multi-modelling approach for profile monitoring of signal data

GRASSO, MARCO LUIGI; COLOSIMO, BIANCA MARIA; Tsung, Fugee

A Phase I Multi-Modelling Approach for Profile Monitoring of Signal Data

Abstract: Many industrial processes exhibit multiple in-control signatures, where signal data vary over time without affecting the final product quality. They are known as '*multimode processes*'. With regard to profile monitoring methodologies, the existence of multiple in-control patterns entails the study and development of novel monitoring schemes. We propose a method based on coupling curve classification and monitoring that inherits the so-called "multi-modelling framework". The goal is to design a monitoring tool that is able to automatically adapt the control chart parameters to the current operating mode. The proposed approach allows assessing which mode new data belong to before applying a control chart to determine if they are actually in control or not. Contrary to mainstream multi-modelling techniques, we propose extending the classification step to include a novelty detection capability, in order to deal with the possible occurrence of in-control operating modes during the design phase that were not observed previously. The functional data depth paradigm is proposed to design both the curve classification and the novelty detection algorithm. A simulation study is presented to demonstrate the performances of the proposed methodology, which is compared against benchmark methods. A real case study is presented too, which consists of a multimode end-milling process, where different operating conditions yield different cutting force profile patterns.

Keywords: Process Monitoring; Multimode Process; Profile Monitoring; Functional Data Classification; Novelty Detection; Functional Data Depth; Quality Control; Manufacturing Processes.

1 Introduction

Traditionally, Statistical Process Control (SPC) relies on the assumption that the process has only one in-control (IC) state, which can be described by a single IC pattern of monitored variables or signals. In the framework of profile monitoring applications (Kang and Albin, 2000; Woodall *et al*., 2004; Colosimo and Pacella, 2010), such a pattern consists of a spatially or time-ordered waveform known as "*profile*". Different authors (Colosimo and Pacella, 2010; Jin and Shi 2001; Chang and Yadama, 2010; Grasso *et al*., 2014, Chou *et al*., 2014) showed that the IC shape of the monitored profile might be considered as a 'signature' of the manufacturing process, whose stability over time is related to the quality of the process itself. Nevertheless, many real industrial processes exhibit more than one IC state (Zhao *et al*., 2010; Ge *et al*., 2013; Xie and Shi, 2012), due to the existence of multiple operating conditions (i.e., different sets of working conditions, different machine settings after shutdown, different tool copies, etc.). In this case, a single profile is not sufficient to fully characterise the process, since the IC state may be described in terms of multiple signatures, all of them corresponding to acceptable quality parts. This is particularly relevant when profile monitoring techniques are applied to signal data, as sensor signals are usually highly affected by changing operating conditions. In the presence of multiple IC signatures, the term '*multimode process*' is used (Wen *et al*., 2015; Ren *et al*., 2015; He and Xu, 2016; Zhao *et al*., 2010; Ge *et al*., 2013; Xie and Shi, 2012). A multimode process is a process that switches from one IC operating mode to a different one, producing a stream of data from different IC distributions (or waveforms). SPC of multimode processes in discrete-part manufacturing was studied in a recent paper (Grasso *et al*., 2015), which focused on the comparison of nonparametric techniques where quality features of interest are simple variables and not profiles. Profile monitoring of multimode processes was recently proposed for geometric shape monitoring (Park and Shrivastava, 2014). In that case, the authors used a mixture of time-series models to characterise the sequence of geometric observations under in-control process conditions. Compared to that study, this paper presents a different perspective, which tries to combine effectiveness and ease of use. Instead of modelling the multimode process dynamics, the so-called '*multi-modelling*' paradigm (Xie and Shi, 2012; Ge and Song, 2009; Zhao *et al*., 2004) is applied and extended to the profile monitoring framework. The multi-modelling approach involves a database of historical IC data to design mode-specific control charts, i.e. one distinct chart for each mode. This implies a two-step procedure: (i) a classification step, aimed at determining which mode new data belong to, among the ones already included in the database, and (ii) the application of control charts to determine if the process remained IC over the period of time where profile data were collected. However, when an unexpected modification of the operating mode occurs under IC conditions (i.e., when a full recording of covariate information is not available in advance), the existing methods may not be able to signal the change. As a matter of fact, any classification algorithm identifies the mode, among the ones included in the database, that better matches the current observations. However, if none of the known modes actually represent the current process state, the algorithm is forced to yield a match anyway. When this happens during Phase I, a wrong estimation of control chart parameters may take place, leading to detrimental effects on process monitoring performances. New IC states, which were not observed in the past, may occur during the process lifecycle, and different authors (Zhao *et al*., 2010; Xie and Shi, 2012) pointed out the importance of coping with the so-called “new mode development”. Nevertheless, the literature still lacks formalized strategies on how to deal with it.

The aim of this study is to provide the practitioner with a support tool able to: i) avoid misclassification errors during the multi-modelling control chart design (a.k.a. Phase I), and ii) automatically signal the possible occurrence of novel modes during the collection of data that should be representative of IC conditions. Since a classification step is not able to deal with new IC states, we propose to couple it with a so-called ‘*novelty detection*’ step (Markou and Singh, 2003; He and Girolami, 2004). Novelty detection methods are classification techniques aimed at determining if a set of data belongs to one of the available classes or whether it represents a brand new class. When the current observations are classified as a '*novelty*', a warning is automatically signalled. Then, one has to decide whether they represent a new IC mode or whether they are the realisation of an out-of-control (OOC) state. Such a decision requires a retrospective investigation, aimed at finding the assignable causes for the observed data.

In order to deal with profile data, we propose the use of the *functional data depth* methodology (Fraiman and Muniz, 2001; Cuevas *et al*., 2007) for both classification and novelty detection. Functional data depth allows the measuring of how internal a profile is with respect to a reference set of curves. It represents a generalisation of multivariate depth methods (Tukey, 1975) to functional data. One major benefit consists of it being suitable to compare profile patterns in different modes without defining a common modelling framework.

The present study contributes to the existing literature by i) extending the multi-modelling framework to profile monitoring applications, ii) integrating classification an novelty detection to cope with new mode development and iii) demonstrating the effectiveness of the functional data depth methodology to enhance classification performances. A real industrial application in end-milling operations is first presented to discuss the method from a practical implementation viewpoint in a real multimode profile monitoring problem. A simulation study is then presented to demonstrate the performances of the proposed approach and to compare it against other benchmark methods for curve classification.

Section 2 presents the proposed methodology; in Section 3 the real case study in end-milling is discussed; Section 4 presents the simulation study and the results of the comparison analysis; Section 5 concludes the paper.

2 Methodology

2.1 The multi-modelling framework

Recent studies devoted to multimode processes in the field of both univariate and multivariate control charts mainly focused on two approaches (Zhao *et al*., 2010; Ge *et al*., 2013), namely the global modelling approach (Lane *et al*., 2001; Hwang and Han, 1999) and the multi-modelling approach (Choi *et al*., 2005; Ge and Son, 2009; Zhao *et al*., 2004). Both the methods assume the availability of a database that characterises the natural process behaviour in known operating modes (these methods are also known as 'model-library methods' (Ge *et al*., 2013)). Nevertheless, they make different uses of the information included in the database. The global modelling approach consists of designing a single control chart that is globally able to monitor the process in every known state: this means that the entire database, without any distinction between different modes, is used to design the chart (Grasso *et al*., 2015). The multi-modelling approach, instead, consists of designing one control chart for each IC mode, such that only the information related to the IC state that matches the current observations is used for the end-use monitoring phase. This study is devoted to the multi-modelling paradigm. The occurrence of new IC modes is more likely during Phase I, when data collection in multiple operating modes is needed to build an historical database of IC patterns. Thus, this study focuses on the multi-modelling control chart design phase.

PLEASE, INCLUDE FIGURE 1 ABOUT HERE

Accordingly to the methods proposed in the literature (Zhao *et al*., 2010; Xie and Shi, 2012; Choi *et al*., 2005; Ge and Song, 2009; Zhao *et al*., 2004; Chu *et al*., 2004; Srinivasan *et al*., 2004; Wang *et al*., 2012; Zhu and Song, 2012) the Phase I procedure can be schematized as shown in Fig. 1 a). Assume that a non-empty database is already available at some given point in time. Then, a new process run is performed and signal data are collected. A classification step is applied to determine which IC mode they belong to, among the ones included in the database. Once a match has been found, the new dataset is added to the corresponding historical dataset to update the control chart parameters and to determine if the process remains IC in its current operating mode. Eventually, the database may be updated by including the new observations from the current state (if they are IC), and the new control chart parameters can be saved. However, there is no formalized procedure to deal with the occurrence of operating modes that do not belong to the available database. As a matter of fact, classification algorithms assume that the current observations originate from one of the known modes in the database. In the presence of a new IC state the expert is not aware of, a misclassification may lead to a wrong estimation of control chart parameters, with detrimental effects in terms of both Type I and Type II errors. In order to avoid this limitation and to provide the practitioner with a support tool that automatically signals possible novel modes, we propose a more general approach, schematised in Fig. 1 b). The classification step is replaced by a *classification and novelty detection step*. When the current observations match a mode included in the database, the basic approach shown in Fig. 1 a) is applicable. When the current observations are classified as a '*novelty*', instead, a warning is signalled and one has to decide whether these observations represent a new IC mode or whether they are the realisation of an out-of-control (OOC) state (i.e., an unnatural pattern). Such a decision requires a retrospective investigation, aimed at finding the causes for the observed novelty, which is equivalent to the search for assignable causes in traditional SPC schemes. However, in the presence of multimode processes, the decisional process includes three possible explanations for the observed alarms: i) the process has not changed (i.e., the signal was caused by the natural process variability), ii) the process has shifted towards an OOC state, iii) the process has shifted towards a novel IC state. In this framework, the practitioner in charge of searching for assignable causes should consider any possible change in the operating condition of the system, starting from a visual inspection of data patterns[*]. If the outcome of this investigation is that a new IC mode has occurred, the database is updated. A control chart for the current mode can be designed and used in a retrospective way to determine if new data are actually IC or not. However, the novelty detection step allows the signalling of a pattern variation at the beginning of a new data collection, whereas, in traditional SPC, potential OOCs can be signalled only after all design data are collected, when the Phase I control chart is applied in a retrospective way. This is expected to ease the investigation analysis, because the time interval between the occurred event and the signal is shortened.

During Phase II, the method works in the same way, but the control chart parameters are kept fixed. If the new process data are classified in one known mode, the corresponding control chart is activated to monitor the process. If the new data are classified as a novel mode, a warning is signalled and a search for assignable causes is called.

[*] As an example, during a milling process, possible sources of a process state modification include: change in machine tool configuration or calibration, change of environmental conditions, modification of part fixturing, changes of material, tools, equipment, cutting parameters, etc.

As far as profile monitoring applications are concerned, both the classification and the novelty detection step rely on functional data analysis (FDA) (Ramsay, 2006) to characterise and compare profile data patterns. The use of a common formalism to solve both the steps is expected to increase efficiency and to ease the implementation of the overall method. To this aim, we propose the use of the *functional data depth* technique (Fraiman and Muniz, 2001; Cuevas *et al*., 2007), which is a measure of how internal a profile is with respect to a reference set of curves. With regard to multimode processes, such a nonparametric approach is expected to provide higher flexibility, as the variety of profile shapes imposed by different IC modes may complicate the choice of a common modelling framework (see Section 2.2 for further details). The potentials of functional data depth for classification purposes were investigated by different authors (Lopes-Pintado *et al*., 2010; Li *et al*., 2012), although its use for novelty detection has not been explored thus far.

The proposed approach relies on two assumptions that are coherent with actual industrial applications and shared by most mainstream methods for multimode process monitoring. The first assumption is that the process consists of sequential runs: within each run, the process remains stable unless an OOC event occurs. This implies that each mode is assumed to persist for a period of time[†]. On the contrary, different runs may correspond either to different operating modes or to replicates of the same mode. This assumption allows one to apply the classification and novelty detection step only at the beginning of a new process run execution. The second assumption is that transitory phases between consecutive runs or consecutive operating modes are not monitored, because

[†] In the presence of quickly and randomly changing modes, the global modelling framework could be preferred to the multi-modelling one.

their transient nature is not compatible with classical SPC principles (although a few authors proposed methods to monitor them as well (Zhao *et al*., 2010)).

2.2 Problem formalization

Let $\{\boldsymbol{Y}_1, \boldsymbol{Y}_2, \dots, \boldsymbol{Y}_j, \dots\}$ be a temporal sequence of sampled profiles originated from the process in its current state, such that $\boldsymbol{Y}_j = [Y_{j,1}, Y_{j,2}, \dots, Y_{j,p_j}]^T$ is the j^{th} profile of sample size p_j, $j = 1,2, \dots.$, which is associated to a complete cycle of an operation. Without loss of generality, assume a constant size for all the profiles, i.e., $p_1 = \cdots = p_j = \cdots = p$. Each profile, $\boldsymbol{Y}_j$, can be treated as a sampled realisation of a functional form, i.e., a square integrable real valued function $Y_j(t) \in L^2([0, T])$ defined over the time interval $[0, T] \subset \mathbb{R}$‡. Then, let $Y_j^{(l)}(t)$ be the j^{th} profile realisation in the current process state (either IC or OOC), where the current mode is denoted by the superscript 'l'. Let $\boldsymbol{Y}_{IC} = \{Y_1^{(h)}(t), \dots, Y_{J_h}^{(h)}(t): h = 1,2, \dots, H\}$ be a multimode historical IC database, where $H \geq 0$ is the number of known IC modes, each of them consisting of a historical collection of J_h IC profiles, $h = 1, \dots, H$. For simplicity of exposition, assume that $J_1 = \dots = J_H = J$.

The proposed approach for multi-modelling control chart design consists of the following steps:

- *Step 1*: when a new process run is performed, a small number $M \geq 1$ of preliminary observations $\left\{Y_1^{(l)}(t), \dots, Y_M^{(l)}(t)\right\}$ are acquired and compared with the profile patterns included in the database, $\boldsymbol{Y}_{IC} = \{Y_1^{(h)}(t), \dots, Y_J^{(h)}(t): h = 1,2, \dots, H\}$, to

‡ In this study we refer to in-process monitoring applications, where profile data are time-ordered waveforms extracted from sensor signals; however, the same approach can easily be extended to geometric profiles.

determine if: (a) the current state matches one of known IC modes or (b) it is a new mode (either IC or OOC); this step is referred to as '*multimode classification and novelty detection*'; if option (a) is applicable, go to step 2, otherwise step 3 is applied;

- *Step 2*: profile data in the current mode are collected, say $Y_1^{(l)}(t), \dots, Y_N^{(l)}(t)$, where $N > M$, and queued to the J past profile data available in the database; then, a suitable control charting method for profile data is applied to the set of $N + J$ realisations: if they are IC, the database is updated by adding the new N profiles, otherwise an alarm is signalled and a search for assignable causes is started;
- *Step 3*: in the presence of a new mode, a retrospective investigation is carried out to determine if it is an IC mode or an OOC mode (this step is usually performed in industrial quality control and it assumes the availability of an expert that supervises the process, though an automatic implementation of this step may be studied in future research); if it is an OOC mode, an alarm is signalled and data in the current run are not used to update the database, otherwise step 4 is applied;
- *Step 4*: profile data in the new IC mode are collected, say $Y_1^{(l)}(t), \dots, Y_N^{(l)}(t)$, where $N > M$, and a suitable control charting method is applied to determine if the process remained IC over the period of time where those data were collected. If no OOC state is detected, the new data are used to update the IC database by adding the $(H + 1)^{th}$ mode.

Section 2.2 briefly introduces the functional data depth formalism and the rationale for its usage, whereas Section 2.3 describes the proposed approach for profile classification and novelty detection. In Section 2.4, we finally discuss the control chart design and use.

2.3 Functional data depth

The notion of data depth was proposed to generalise order statistics to higher dimensions (Tukey, 1975). In multivariate data analysis, it is used to determine the degree of centrality of a point within a data cloud, with a particular regard to nonparametric problems (the higher the depth, the more internal is the point). Such a notion has been extended to the FDA framework (Fraiman and Muniz, 2001; Cuevas *et al*., 2007; Lopes-Pintado and Romo, 2007) to measure the centrality of a curve within a set of curves. Such a centrality measure can be used as a similarity index without fitting any model to the profiles, which is expected to provide great flexibility in this framework.

Different functional data depth formulations were proposed in the literature. They include the *Fraiman and Muniz depth* (FMD) (Fraiman and Muniz, 2001), the *w-modal depth* (MD) (Cuevas *et al*., 2007), the *Random projection depth* (RPD) (Cuevas *et al*., 2007) and the *Multi-Band Depth* (MBD) (Lopes-Pintado and Romo, 2007). The RPD formulation works by projecting the functional data and their derivatives along a given number of random directions, which increases the computational effort with respect to other formulations (Febrero *et al*., 2008). Thus, in this study only the FMD, the MD and the MBD are considered. The simulation analysis discussed in the following will show that the MD technique outperforms the others in terms of profile classification performances, and hence it is considered as the baseline formulation.

Consider a generic square integrable real valued function $Y_j(t) \in L^2([0,T])$ defined over the time interval $[0,T] \subset \mathbb{R}$, where $j = 1,2,\ldots$. Then, the MD technique is based on computing to what extent a given curve is densely surrounded by the rest of the curves, as follows (Cuevas *et al*., 2007):

$$D_j(n) = \sum_{k=1}^{n} K\left(\frac{\|Y_j(t) - Y_k(t)\|}{S}\right), \qquad j = 1,2,\dots \tag{1}$$

where $\|\cdot\|$ is a norm in the functional space, $K(\cdot): \mathbb{R}^+ \to \mathbb{R}^+$ is a kernel function and S is the kernel bandwidth. The curve that maximises the data depth is the one most densely surrounded by the n curves belonging to the dataset. Cuevas *et al*. (2006) recommended using either a L^2 or a L^∞ norm, and a truncated Gaussian kernel:

$$K(t) = \frac{2}{\sqrt{2\pi}} \exp\left(-\frac{t^2}{2}\right), \qquad t > 0 \tag{2}$$

with bandwidth $S = 0.2\max\{\|Y_{k1}(t) - Y_{k2}(t)\|: k1, k2 = 1, \dots, n\}$. Febrero *et al*. (2008) highlighted that the MD measure is robust with respect to the choice of the bandwidth parameter. The above kernel choices are used in this study, as they were proved effective in practice. Future studies may be aimed at investigating in more detail the effect of those choices on multimode profile monitoring performances. The FMD and the MBD formulations are briefly described in Appendix A.

The functional data depth methodology allows designing nonparametric classifiers for profile data, avoiding the need for a modelling framework that is common to every observed mode. Classification methods for functional data are usually extensions of their multivariate counterparts, based on the analysis of multivariate vectors of profile model coefficients (Ramsay, 2006). However, in multimode process monitoring applications, the variety of profile shapes that can be observed might entail the use of different modelling frameworks for distinct modes. This reduces the effectiveness of parametric classification algorithms. As an example, Zhao *et al*. (2004) proposed a multimode process monitoring approach based on multiple Principal Component Analysis (PCA) models that could be extended to profile data. Although the PCA represents a common modelling framework, one challenge consists of the fact that different modes may need different numbers of retained principal components to capture equivalent percentages of data variability. One possible way to face such a challenge consists in classifying the curves by looking at model residuals instead of model coefficients (Zhao *et al*., 2004). However, residual-based classification performances are often not fully satisfactory, as will be shown in the rest of the paper.

Nonparametric classification is therefore a suitable category of methods to deal with classification problems in the frame of multimode processes. Among them, data depth-based techniques are particularly attractive as they do not need defining a template to compare to, contrary to most similarity-based methods. A simulation study to compare different classification and novelty detection methods is discussed in Section 3.

It is worth noting that when the data depth concept started to be taken into account for SPC applications a few years ago, criticism involved the high computational costs. Nowadays, available technology makes this technique feasible and comparable to other multivariate or functional methods. As an example, the CPU time[§] to compute the MD functional depth of a single profile of size $p = 100$ with respect to $n = 50$ past profiles of equal size was about $0.05\ s$ by using an R implementation of the code.

2.4 Multimode classification and novelty detection

Some authors investigated the use of data depth measures for functional data classification (Lopes-Pintado and Romo, 2007; Febrero *et al*., 2008), but the basic classification problem does not envisage the possibility that none of the available classes match the current sample. Very few studies were devoted to the coupled task of classification and novelty detection (sometimes synthetically called '*multi-class novelty*

[§] On an Intel® Core™ i7-3740QM CPU @ 2.70 GHz *detection*'), either in FDA or in classical multivariate analysis applications. In the FDA framework, Febrero *et al*. (2008) treated the novelty detection problem by using the functional data depth from an outlier detection perspective. For a review of statistical novelty detection methods refer to Markou *et al*. (2003).

The proposed approach consists of solving two sequential problems:

- *Problem 1* (classification): identification of the historical IC mode that better matches the current observations, among the IC modes included in the $\boldsymbol{Y}_{IC}$ database.
- *Problem 2* (novelty detection): assessment, at a given confidence level α_N, of whether the current observations originate from that IC mode or whether they represent a new mode.

For the sake of clarity, first assume that $M = 1$: in this case, the classification and novelty detection decision is based only on the analysis of the first profile acquired in the current process run, i.e., $Y_1^{(l)}(t)$. A data depth-based classification for functional data (known as '*maximum depth approach*') consists of classifying the current observation, $Y_1^{(l)}(t)$, in the IC mode that maximises the functional depth $D_1^{l,h}(J)$ (Cuevas *et al*., 2007), i.e., $\arg\max_h D_1^{l,h}(J)$. If the MD formulation is used, then:

$$D_1^{l,h}(J) = \sum_{k=1}^{J} K\left(\frac{\left\|Y_1^{(l)}(t) - Y_k^{(h)}(t)\right\|}{S}\right) \tag{3}$$

That mode, say $h = \hat{h}$, is then used as a candidate for the next novelty detection step. Some authors proposed other depth-based classification schemes: in particular, Li *et al*. (2012) studied a way to enhance the maximum depth approach by using the depth-versus-depth plot (called '*DD-plot*'), but the high computational cost required to compute cross-mode depth values makes that approach hardly applicable to in-process monitoring applications. Thus, the maximum depth approach is considered in this study.

Once a candidate mode has been identified, denoted by $\hat{h}$, the first step of the novelty detection procedure consists of estimating the empirical distribution of the J depth measures of IC profiles included in $\boldsymbol{Y}_{IC} = \{Y_1^{(\hat{h})}(t), \dots, Y_J^{(\hat{h})}(t)\}$. Let $\hat{F}(J)$ be the empirical distribution of the J depth measures in the candidate mode $\hat{h}$. Then, the detection of a novelty works by comparing the depth $D_1^{l,\hat{h}}(J)$ with the $(1-\alpha_N)\%$ percentile of that empirical distribution, denoted by $\hat{F}_{\alpha_N}(J)$. Since $D_1^{l,h}(J) \in \mathbb{R}^+$ and lower depth values correspond to more external (or dissimilar) profiles, if

$$D_1^{l,\hat{h}}(J) < \hat{F}_{\alpha_N}(J) \tag{4}$$

then, the observation is classified as a realisation generated by a new mode (either IC or OOC), otherwise the result of the classification step is confirmed (i.e., $l \equiv \hat{h}$). The choice of the parameter α_N, where $0 < \alpha_N < 1$ (e.g., $\alpha_N = 0.95$) and the subscript 'N' stands for 'novelty', controls the confidence for such a decision.

Notice that this approach involves estimating the empirical distribution of depth values only for the $\hat{h}$ mode selected after the classification step, which yields computational effort-saving against applying the novelty detection step with no previous classification.

It will be shown that better results can be achieved if a number $M > 1$ is used to decide on the nature of the current process mode. In this case, the above procedure can be iteratively applied to the first M profiles acquired in the current process run, i.e., $\left\{Y_1^{(l)}(t), \dots, Y_M^{(l)}(t)\right\}$. Then, a majority voting approach can be used, either to classify the current process mode as a known IC mode or a brand new one. Majority voting simply consists of selecting the alternative that has the majority, for $j = 1, \dots, M$. In the presence of ties, a random classification can be applied for the current observation; otherwise, a warning can be raised and the tie fixed by using a larger number of samples, M. Majority voting is a consolidated procedure in classification problems, and more sophisticated methods are available in the literature (Hastie *et al*., 2009). In this study, the benefits of a basic majority voting rule are investigated. The development of a tuned procedure may be envisaged in future research. The choice of M is the result of a compromise between the computational effort for classification and novelty detection on the one hand, and the minimisation of the misclassification error on the other hand.

2.5 Control chart design

Once the classification and novelty detection step is over, the following observations in the current mode, $Y_{M+1}^{(l)}(t), Y_{M+2}^{(l)}(t), \dots$, are collected and analysed together with the former M ones. Any control charting scheme suitable to deal with profile data (Woodall *et al*., 2004; Colosimo and Pacella, 2010; Jin and Shi, 2001) can be applied to determine if these observations were IC over the period of time where they were collected. The choice of the most suitable scheme is problem-dependent and is mainly influenced by the nature of the profile pattern. Since a review of profile monitoring approaches is beyond the scope of the present paper, the interested reader may refer to Noorossana *et al*. (2012). In any case, it is possible to draw some general considerations about the use of profile monitoring control charts in the presence of multimode processes. First, the choice of the curve parametrisation approach for control chart design may inherit some possible knowledge about the existence of shared characteristics among different modes in terms of profile patterns (e.g., a common location of salient shape features). In case of cross-mode shared properties, it is advisable to exploit this information to define the modelling framework (e.g., a spline regression basis with common knot locations for every mode). On the contrary, when multiple operating modes yield considerably different profile patterns, independent and mode-specific models might be preferred. Model-free control charts might be chosen too, which need no profile modelling step. For a discussion about nonparametric control charts for profile data the reader is referred to Noorossana *et al*. (2012) and Qiu and Zou (2010). However, the proposed approach imposes no constraint on the choice of the control charting scheme that follows the data classification and novelty detection step. As an example, the use of a PCA-based control chart (Colosimo and Pacella, 2007) is exemplified in the end-milling case study in Section 3 (and briefly reviewed in Appendix A).

A further important consideration regards the alignment of profiles in different modes. In this study, we assume profiles to be naturally aligned, but in most practical applications a registration operation is required. The critical role of curve registration was discussed by different authors (Woodall *et al*., 2004; Colosimo and Pacella, 2007), and the importance of properly integrating the registration information into profile monitoring schemes was highlighted in Grasso *et al*. (2016). In multimode processes, the misalignment of profiles may have a detrimental effect on both the classification and novelty detection results and the following monitoring performances. Some authors showed that curve classification and registration operations may be performed in an iterative way to enhance the outcome (Sangalli *et al*., 2010). Future research should be aimed at addressing this issue.

3 A real case study in end-milling

In order to provide practical guidelines on the use of the proposed approach, a real case study in end-milling is presented. It consists of three sequential end-milling cuts performed on a Ti-6Al-4V part with a rectilinear feed path along the X axis by using a four teeth ATI Stellram porcupine mill (with diameter of $63\ mm$ and length of $180\ mm$) mounting SDTH 120412EN-422 X500 inserts. The three cuts were performed by using the same set of cutting parameters (the ones listed in Table 1), but a tool copy change was applied after cut 1, before cut 2 and 3. The two copies of the tool are labelled as ‘copy 1’ and ‘copy 2’. Tool copy changes are automatically operated when the duration of the process is longer than the tool life, but not necessarily a copy change yields a modification of signal data patterns.

In the first two cuts, the same quality surface finishing on the part was achieved. During the third cut a tool breakage occurred, leading to out-of-control cutting performances. The first two cuts were used in Phase 1, whereas the third cut was used to test the process monitoring performances in Phase II. The machine tool adopted to perform the tests was a five-axis machining centre equipped with a $455\ Nm$, $50\ kW$, $8000\ rpm$ head (the experimental set-up is shown in Fig. 2).

PLEASE, INCLUDE TABLE 1 ABOUT HERE

PLEASE, INCLUDE FIGURE 2 ABOUT HERE

The three components of the cutting force signal were acquired at $2\ kHz$ by means of a Kistler 9255B dynamometer, and the resultant cutting force was used for in-process monitoring purposes. The signal was automatically segmented into repeating profiles by using a tachometric trigger associated to the angular position of the spindle rotor, such that each profile corresponds to a complete spindle revolution. A synchronous re-sampling procedure was also applied to obtain profiles of equal length, $p = 264$, without affecting the relevant frequency content of the signal.

Fig. 3 shows the IC cutting force profiles corresponding to cut 1 (left panel) and cut 2 (right panel). The number of acquired profiles is $J_1 = 20$ in cut 1 and $J_2 = 30$ in cut 2. The time domain $t \in (0,1)$ corresponds to a duration of about $0.24\ s$. Fig. 3 shows that the tool change operation produced a profile pattern modification due to a slight variation of the run-out error condition, i.e., the deviation of insert orientation from the nominal one. The run-out error is a not fully controllable factor, depending on the kind of tool and the industrial practice for tool pre-setting. In this case, the different tool run-out condition impacts the height of local peaks in the cutting force profiles, especially the second and third largest peaks, associated to the second and third cutter, respectively.

Fig. 3 shows that, contrary to the traditional assumption in profile monitoring, a process may exhibit multiple in-control 'signatures', depending on operating conditions that may not be fully controllable by the machine operator (i.e., variations of tool run-out conditions).

PLEASE, INCLUDE FIGURE 3 ABOUT HERE

As far as Phase I is concerned, the proposed approach works as follows. First, profile data in cut 1 were acquired. A profile monitoring control charting scheme is needed to determine if the data are IC or not. To this aim, a well-known approach was used, i.e., the one based on functional PCA proposed by Colosimo and Pacella (2007), briefly reviewed in Appendix A. The number of retained principal components was selected by setting a threshold on the overall explained variability (i.e., at 90%) and the control limits were estimated accordingly to Colosimo and Pacella (2007). The familywise type I error was set at $\alpha = 0.0027$. No violation of the control limits was observed (see Fig. 5), and hence the process was assumed to be IC, and the operating mode labelled as Mode A. Then, profile data in cut 2 were acquired. Assume that $M = 3$, i.e., the classification and novelty detection steps rely on the first three observations of the process run. The functional data depth values of these three profiles with respect to Mode A are respectively $D_1(J_1) = 0.418$, $D_2(J_1) = 0.425$ and $D_3(J_1) = 0.426$ (see Fig. 4). The $(1-95)\%$ percentile of the empirical distribution of data depth values in Mode A is $\hat{F}_{0.95}(J_1) = 2.976$. The depth of these three profiles with respect to Mode A is lower than this value[**], which means that a "new mode" warning is signalled. The search for assignable causes is then performed. In this specific case, the search should start with the visual inspection of acquired profile data, which reveals a local modification of the cutting force pattern that is explainable in terms of changed run-out conditions. Thus, any symptom of an OOC state being absent, the tool copy change can be pointed out as a possible explanation for the observed pattern modification. Because of this, the new profile data stream is classified as a novel IC state and labelled as Mode B. A new control chart is designed for Mode B data and the process is found to be IC (see Fig. 5).

PLEASE, INSERT FIGURE 4 ABOUT HERE

Assuming that Phase I is over, the profile data acquisition in cut 3 was started and Phase II analysis was applied. The functional data depth-based classification was applied to the first $M = 3$ profiles in cut 3 with respect to Mode A and Mode B. All the three profiles were classified as Mode B, and hence the Mode B control chart parameters were selected to monitor the process. Each new observation of the current cut was plotted onto

---

[**] Low depth values correspond to more external profiles.

the control charts and the result is shown in Fig. 5. The quantities on the Y axis are expressed on a logarithmic scale and vertical solid lines separate the design phase (on the left) from the use phase (on the right) of the charts.

PLEASE, INSERT FIGURE 5 ABOUT HERE

A sustained shift of the SPE statistic (see Appendix A for its definition) was signalled starting from the fifth observation in cut 3. This shift corresponds to a gradual, though rapid, departure of cutting force profiles from their IC pattern caused by the tool breakage.

Fig. 6 shows the cutting force patterns in cut 3: the first profiles are stable and their shape resembles the one of Fig. 3 (right panel), then the effect of the tool breakage becomes more and more severe. Tool breakages and chippings are frequent and difficult events to predict in milling processes on hard-to-cut materials like titanium alloys, which implies the need for in-process monitoring capabilities.

PLEASE, INCLUDE FIGURE 6 ABOUT HERE

Now, consider the implementation of the traditional multi-modelling approach. Since no novelty detection capability is provided, the profile data in cut 2 are classified as Mode A. This means that the control chart design phase consists of a mixture of cut 1 and cut 2. In this case, profile monitoring control charts were designed by queuing cut 1 and cut 2 data in a single dataset; the same charts were then used to monitor the profile data in cut 3. Fig. 7 shows the control charts obtained by using this traditional approach.

Fig. 7 shows that a small mean shift of the SPE statistic (see Appendix A) occurred during the design phase, passing from cut 1 to cut 2, although it was not signalled by the chart. The normal practice would require a retrospective investigation, possibly by designing a more effective chart for small shifts or a change-point detection scheme (Zou *et al*., 2009). This implies two drawbacks: (i) the mode change may be detected only after the dataset belonging to the new mode is collected, whereas the proposed approach allows the identification of a mode change at the beginning of the new mode realisation, and (ii) the design of an additional chart to get an insight of the observed pattern requires supplementary efforts.

PLEASE, INSERT FIGURE 7 ABOUT HERE

In terms of fault detection capabilities, the proposed approach (Fig. 5) yields a faster signal of the OOC event. The run length is $RL = 5$ in the proposed approach and $RL = 9$ in the traditional approach. Moreover, the proposed approach is able to signal 91.4% of cut 3 data as OOC, whereas the traditional approach signals 81.4% of profiles as OOC. This result is due to the inflation of control limits in Fig. 7, caused by a missed separation of Mode A and Mode B during the design phase. Therefore, a rapid identification of a mode change via curve classification and novelty detection is expected to provide the practitioner with an automated support tool to keep under control manufacturing processes in the presence of changing operating modes. The reduction (or even the avoidance) of misclassification errors is expected to enhance the performances of the resulting control charts both in terms of Phase I and Phase II errors. A more extended investigation of the performances provided by our proposed approach is discussed in the next Section via simulation study and comparative analysis.

4 Simulation study

The performances of the proposed classification and novelty detection methodology are demonstrated by using two different models for the generation of multimode patterns. The first scenario is representative of profile data characterised by a simple pattern but a considerable within-mode amplitude variability. The second scenario is representative of more complicated profile data with local pattern differences between different modes. Subsections 4.1 and 4.2 present the simulation study results in these two scenarios, respectively. Subsection 4.3 presents a discussion about the effects of either a lack of mode classification or a mode misclassification on the type I error performances in profile monitoring.

4.1 Scenario 1

In scenario 1, a benchmark model inspired by the work of Tang and Muller (2008) was used. Synthetic profile data are generated by using a model defined as follows:

$$Y_j(t) = \sum_{i=1}^{5} \beta_{i,j} \exp\left\{\gamma_{i,j}\left(t + \omega_{i,j}\right)^2\right\} + \varepsilon_j(t),\ 0 \leq t \leq 1 \text{ and } j = 1,2, \ldots \quad (5)$$

with parameters $\boldsymbol{\beta}_j = [\beta_{1,j}, \ldots, \beta_{5,j}] \sim MN[\boldsymbol{\mu}_\beta, \boldsymbol{\Sigma}_\beta]$, $\boldsymbol{\gamma}_j = [\gamma_{1,j}, \ldots, \gamma_{5,j}] \sim MN[\boldsymbol{\mu}_\gamma, \boldsymbol{\Sigma}_\gamma]$ and $\boldsymbol{\omega}_j = [\omega_{1,j}, \ldots, \omega_{5,j}] \sim MN[\boldsymbol{\mu}_\omega, \boldsymbol{\Sigma}_\omega]$. The noise terms $\varepsilon_j(t) \sim N(0, \sigma_\varepsilon)$ is such that $\sigma_\varepsilon = 0.05$. The following parameter settings were used:

- $\boldsymbol{\mu}_\beta = [0.50, -0.50, 0.60, 0.60, -0.50]$, $\boldsymbol{\Sigma}_\beta = diag[(8.8,5.0,6.0,6.0,5.0)e^{-2}]$
- $\boldsymbol{\mu}_\gamma = [-20, -50, -100, -150, -200]$, $\boldsymbol{\Sigma}_\gamma = diag[2,5,10,15,20]$

With regard to the parameter $\boldsymbol{\mu}_{\omega}$, different settings were used to simulate multimode patterns, being fixed $\boldsymbol{\Sigma}_{\omega} = diag[(5.0,4.5,3.0,2.0,1.5)e^{-2}]$.

Two datasets were generated, based on the same model structure (Eq. 5). The first is a database which comprises profile data from four different IC modes, denoted by Mode A, B, C and D. The second is a testing dataset, which comprises either profile data originated from the aforementioned modes or profile data belonging to different modes, denoted by Mode E, F, G and H. All the simulated modes share the same generating model (Eq. 5), but with different settings of the parameter $\boldsymbol{\mu}_{\omega}$, as shown in Table 2. The multimode profile patterns are depicted in Fig. 8.

PLEASE, INCLUDE TABLE 2 ABOUT HERE

When the testing set includes profile realisations generated from one of the historical IC modes (Modes A, B, C and D), the classification capability can be tested. When, instead, the testing set includes profile realisations from different modes (Modes E, F, G and H), the novelty detection capability can be tested. The results presented hereafter refer to a number $J = 50$ of IC profiles in historical modes. Statistically equivalent results were achieved for larger values of J. Because of this, for the sake of space, only the results related to the choice $J = 50$ are presented and discussed.

PLEASE, INCLUDE FIGURE 8 ABOUT HERE

Different competitor methods could be considered to evaluate the pros and contras of the proposed approach. The competitors considered in this study include: (a) the same method based on different data depth formulations, i.e., the FMD and the MBD formulations (see Appendix B), (b) the same method based on similarity index maximisation, where the L_2 distance is used instead of the functional depth measure, (c) a benchmark classification approach based on the k-Nearest Neighbour (kNN) method (Hastie *et al*., 2009), and (d) a benchmark classification approach based on the Principal Component Analysis (PCA) (Zhao *et al*., 2004). The competitor method (b), denoted by 'L_2', consists of classifying the current observations by minimising the L_2 distance with respect to the profile data in the IC database, and then by comparing the distance between current observations and historical IC profiles with the empirical distribution of the L_2 distances of historical profiles belonging to the candidate mode for novelty detection. The competitor method (c), denoted by '*kNN*', consists of classifying the current observations in the IC mode of their k most similar curves, where the L_2 distance is used as a dissimilarity index. The novelty detection step works analogously to the L_2 approach. The kNN algorithm is known to be a benchmark approach in functional data classification (Lopes-Pintado and Romo, 2010), and the choice of the optimum value of parameter k is based on cross-validation (Wasserman, 2006). The competitor approach (d), denoted by '*PCA*', consists of fitting a PCA model in each known IC mode, and then approximating the current observations by each of those models: the current observations are preliminarily classified in the IC mode that yields the minimum square prediction error (SPE). This approach was proposed by Zhao *et al*. (2004), and is used in this study as a benchmark that represents model library-based approaches. Notice that this approach can be easily extended to functional data and it allows classifying curves regardless of possibly different numbers of PCs required in different modes. However, as no automatic procedure for new mode detection was proposed, the novelty detection step was implemented by comparing the current SPE with the empirical distribution of SPE values in the candidate mode.

The classification performances and the novelty detection performances are depicted in Fig. 9 and Fig. 10, respectively, where the proposed approach is simply denoted by 'MD'. The misclassification and novelty detection errors were computed by evaluating 1000 test runs by randomly generating both IC profiles and testing profiles. The results shown in Fig. 9 and Fig. 10 correspond to the choice $M = 1$, i.e., to the use of one single profile in the testing set for both classification and novelty detection purposes (examples of performances achieved by setting $M > 1$ are discussed below).

Fig. 9 shows that the best classification performances are provided by the benchmark approach based on the kNN technique together with the proposed approach based on MD functional depth. The two approaches provide statistically equivalent results at 95% confidence level. The other two functional depth formulations, i.e., the FMD and the MBD formulations, provide worse results, especially for Mode A, B and D. In this frame, the MD approach is believed to outperform other functional data formulations thanks to the kernel trick adopted in estimating to what extent a curve is densely surrounded by other curves. The FMD is less effective than the MD as it simply consists of an integration of univariate depths at each curve location. The MBD performs better than the FMD in Scenario 1, thanks to the graph-based depth measure, but it is outperformed by the MD in most cases.

The L_2-based approach provides quite good results, but they are comparable with the ones yielded by the proposed MD-based approach and the kNN-based approach only for Mode D. With regard to the PCA-based approach, two threshold levels for the explained variability were considered to select the number of retained components, i.e., 80% and 90%, respectively. Fig. 9 shows that this approach performs quite poorly, especially for Mode B, and it is particularly sensitive to the number of retained components. The reason is that the SPE alone is not a sufficiently reliable statistic for functional data classification purposes. Generally speaking, the misclassification performances depend on two factors: i) the dissimilarity between the average patterns in two (or more) different modes, and ii) the natural variability of the profile patterns within each mode. As an example, mode G was mainly misclassified as Mode B, because of a reduced average dissimilarity between these two modes together with large variability in Mode G, especially in the central portion of its domain. Mode H, instead, is characterised by an average pattern that is quite dissimilar from any other pattern in the dataset. Moreover, its natural variability is such that the probability of a misclassification with respect to most of the considered methods is low.

PLEASE, INCLUDE FIGURE 9 ABOUT HERE

Fig. 10 shows that the proposed MD-based approach outperforms other competitors in detecting novel modes. The L_2-based and the kNN-based methods yield similar results as they share the same similarity index, but they provide higher errors than the MD-based method at least for Mode E and G. Other functional depth formulations, together with the PCA-based approach, provide considerably worse results, leading to very limited novelty detection capabilities.

PLEASE, INCLUDE FIGURE 10 ABOUT HERE

Fig. 9 and Fig. 10 show the results when the classification is based on a single observation, i.e., the case with $M = 1$. As mentioned before, the use of a larger number of profiles, i.e., $M > 1$ may be recommended to achieve better results via majority voting. As an example, Fig. 11 (left panel) shows the misclassification error for different values of M in the range $M \in [1,15]$, for Mode A, and Fig. 11 (right panel) shows the novelty detection error for the same values of M, for Mode E. Fig. 11 shows that both the misclassification and novelty detection errors may be reduced when a majority voting approach is used with $M > 1$.

PLEASE, INCLUDE FIGURE 11 ABOUT HERE

4.2 Scenario 2

In Scenario 2, the multimode profile patterns were generated by using the following model:

$$Y_j(t) = \sum_{i=1}^{8} A_i g_i(t; \mu_i, \sigma_i) + \varepsilon_j(t), \quad j = 1{:}J, t \in (a, b) \tag{6}$$

where the terms $g_i(t; \mu_i, \sigma_i)$ are normal probability density functions with parameters listed in Table 2, $A_i \sim NID(10,0.5)$ is the random amplitude term, and $\varepsilon_j(t) \sim NID(0,0.025)$. The simulated profiles consist of $n = 200$ equispaced datapoints over the interval $t \in (0,1)$.

Two datasets were generated in this case as well, based on the same model structure (Eq. 6). The first dataset comprises profile data from four different IC modes, denoted by Mode A, B, C and D. The second is a testing dataset, which comprises either profile data originated from the aforementioned modes or profile data belonging to different modes, denoted by Mode E, F, G and H. All the simulated modes share the same generating model (Eq. 6), but with different settings of the parameter μ_i and σ_i, as shown in Table 3. The multimode profile patterns in Scenario 2 are depicted in Fig. 12.

PLEASE, INCLUDE TABLE 3 ABOUT HERE

PLEASE, INCLUDE FIGURE 12 ABOUT HERE

The classification performances and the novelty detection performances are depicted in Fig. 13 and Fig. 14, respectively. The same simulation settings described in subsection 3.1 were also applied to Scenario 2.

PLEASE, INCLUDE FIGURE 13 ABOUT HERE

Fig. 13 shows that the MD, MBD, L_2 and kNN methods yield no misclassification error for modes A, B, C and D. The FMD and the PCA-based classification with explained variability threshold at 80% yield the worst results, especially in the presence of mode A, B and D. However, all the methods provide quite good classification performances, as the average misclassification error is always lower than 2%. This is caused by the fact that the within-mode amplitude variability in Scenario 2 is lower than the variability in Scenario 1, which eases the mode separation even in the presence of local shape differences.

Regarding the novelty detection performances, Fig. 14 confirms that the FMD and the PCA methods yield the worst results. The FMD-based approach is not able to identify modes E, G and H as novel modes, whereas the PCA-based approach is not able to identify modes F, G and H as novel modes. All the other methods yield good novelty detection performances, especially the ones based on the MD, the L_2 distance and the kNN algorithm.

PLEASE, INCLUDE FIGURE 14 ABOUT HERE

These results confirm that the FMD method, which is a simple extension of univariate data depth estimation to functional data, may not be a suitable choice for multimode classification and novelty detection of profile data. The MBD approach is more effective than the FMD in Scenario 2, but the simulation results in Scenario 1 showed that the MD approach may outperform both the FMD and the MBD. Moreover, the SPE statistic used in PCA-based methods is not a sufficiently reliable statistic for functional data classification purposes. Generally speaking, the best competitor of our proposed approach is represented by the kNN-based algorithm, although the use of the MD metric seems to be more effective than the L_2 distance used by the kNN, at least for novelty detection purposes.

4.3 Misclassification effect on type I error performances

In the presence of multimode patterns, the performances of profile monitoring control charts may be strongly affected either by a lack of classification capabilities or by a misclassification between different IC modes. The objective of the analytical study presented here consists of quantifying this effect via Monte Carlo simulations. To this aim, the same monitoring scheme used in Section 3 was used, i.e., the one based on functional PCA proposed by Colosimo and Pacella (2007), briefly reviewed in Appendix A. A number of principal components that globally capture at least 90% of data variability were retained in each mode, and the corresponding scores were monitored via a Hotelling's T^2 control chart. The information content captured by the remaining principal components was monitored via the SPE statistics. A familywise type I error $\alpha = 0.01$

was set and empirical control limits were estimated. The simulation involved 100 runs; each run consists of $M = 1100$ profiles for control chart design and $N = 5000$ profiles as testing dataset. The M profiles were divided into two sets: a set of $M_1 = 100$ profiles was used to estimate the PCA model, and the remaining $M_2 = 1000$ profiles were used to estimate the empirical control limits. Two different cases were tested for both Scenario 1 and Scenario 2. In the first case, the design phase includes profiles from modes A, B, C and D in equal proportions, whereas, in the second case, the design phase consists of one single mode ranging from mode A to mode D. In both cases, the testing phase includes one single mode, ranging from mode A to mode D. Thus, the first case is representative of a control chart design that lacks any multimode classification capability, where Phase I includes a mixture of multimode patterns. The second case, instead, is used to study the effect of a mode misclassification on control chart performances, i.e., a chart designed by using data from one IC mode and then applied to monitor the process in another IC mode.

In both cases, the control chart performances were characterised in terms of the type I error, i.e., in terms of false alarm rates. Table 4 shows the 95% confidence intervals for the type I errors for the different cases considered in Scenario 1 and Scenario 2. Table 4 shows that a lack of multimode classification (i.e., when the design phase consists of a mixture of modes) may yield false alarm rates that are lower (e.g., see Mode A in Scenario 2) or greater (e.g., see Mode B in Scenario 2) than the target one, depending on the mode included in the testing set. This means that a mixture of modes may either inflate the control limit estimate, with detrimental results in terms of type II errors, or increase the false alarm rate. In the presence of a mode misclassification (case 2), instead, the false alarm rate is always increased: it can be up to ten times greater than the target type I error. Analogous results were achieved both in Scenario 1 and Scenario 2. These results highlight that neglecting the multimode nature of profile data in traditional control charting schemes may yield monitoring performances that are considerably far from the desired ones. On the other hand, a mode misclassification may strongly inflate the false alarm rate, which motivates the need for effective classification and novelty detection techniques.

PLEASE, INCLUDE TABLE 4 ABOUT HERE

5 Conclusion

Many industrial processes exhibit multiple operating conditions that yield natural transitions between multiple IC states. This represents a violation of common SPC assumptions and entails the development of novel monitoring procedures. Recent studies devoted to chemical process engineering pointed out the actual industrial relevance of multimode processes. This paper presented a methodology to design control charts for profile data in the presence of multimode patterns. The study extends the so-called 'multi-modelling framework' that involves two sequential steps, i.e., a classification step and a control charting step. The classification step is aimed at determining which mode new data belong to in order to apply the following control charting scheme by using only the information that is relevant to the current process state. Previous studies devoted to this approach lack formalized strategies to deal with the occurrence of new modes, i.e., operating modes that were not previously observed. In order to cope with this limitation, a generalisation of the classification step is proposed to include a novelty detection capability. This allows assessing whether the current observations match one mode included in the historical database or whether they should be treated as a new mode. When a novel state is detected, a retrospective analysis should be performed to determine if the novel state is IC or not. Analogously to traditional SPC, such an investigation may be carried out by the expert who supervises the process, although its automatic implementation may be the subject of future studies. Both the classification and the novelty detection steps can be based on the functional data depth paradigm, which can be applied without the need for a common modelling framework shared by distinct modes. The aim is to provide the practitioner with a support tool able to automatically signal operating mode changes and to reduce (or even avoid) misclassification errors that could affect the process monitoring effectiveness. The occurrence of undetected new modes in Phase I is highly critical as it affects the estimation of the control chart parameters in different modes. Because of this, a Phase I procedure is proposed, but the multi-modelling approach can be extended to Phase II as well.

The simulation study demonstrated that the proposed depth-based approach outperforms most competitor and benchmark techniques for both classification and novelty detection. The simulation analysis suggested that a majority voting scheme could enhance the classification performances by comparing a number $M > 1$ of first profile data from the current process run with the ones in the IC database. The choice of M is expected to be the result of a compromise between the computational effort required by the classification and novelty detection step on the one hand, and the misclassification error minimisation on the other. Future studies may further investigate the role played by majority voting algorithms, and their impact on overall performances.

A real case study in end-milling was presented to discuss the proposed approach from a practical implementation viewpoint in a real multimode profile monitoring problem. The case study showed that the lack of a novelty detection capability may cause a wrong mixture of data from different operating modes into a single class, with detrimental effects in terms of control chart performances.

Eventually, in this study we assumed that the monitored profiles are already registered or do not need registration. Such an assumption may hardly be applicable in practice (e.g., see Grasso *et al.*, 2016), and hence, a generalisation of the proposed method to cope with multimode misaligned profiles may be the subject of a future study.

Abbreviations and nomenclature

ARL, ARL_0	Average Run Length and IC Average Run Length
$B(\cdot)$	Band defined by a set of functional curves
CC	Control Chart
$D_j^{l,h}(\cdot)$	Functional data depth of j^{th} profile in l^{th} mode with respect to profiles in h^{th} mode
FDA	Functional Data Analysis
FMD	Fraiman and Muniz Depth
$G(\cdot)$	Graph of functional curve
h	Index of known modes in historical dataset, $h = 1, \dots, H$
$\hat{h}$	Candidate mode
IC	In-Control
j	Profile index, $j = 1,2, \dots$
J	Number of profiles in each mode of the $\boldsymbol{Y}_{IC}$ database
k	Number of nearest neighbours used in kNN benchmark approach
$K(\cdot)$	Kernel function
kNN	k-Nearest Neighbour
l	Mode index, $l = 1,2, \dots$
L^2	Distance used as dissimilarity index
M	Duration of warm-up phase
MBD	Multi-Band Depth
MD	Modal Depth
n	Number of historical IC samples
OOC	Out-of-Control
p	Length of acquired profiles

PCA	Principal Component Analysis
Q	Tuning parameter used in Eq. A3
RL	Run length
RPD	Random Projection Depth
S	Kernel bandwidth
$S_{n,q}(\cdot)$	Proportion of bands $B(\cdot)$ determined by q different curves containing a given graph
SPC	Statistical Process Control
SPE	Square Prediction Error
t	Time index ($t \in [0, T]$)
$\boldsymbol{Y}_j^{(l)}$	j^{th} profile acquired in l^{th} mode, $j = 1,2, \ldots$ (denoted by $Y_j^{(l)}(t)$ in functional form)
$\boldsymbol{Y}_{IC}$	Database of multimode IC profile data
α	Target Type I error
α_N	Confidence level used for new mode detection
$\boldsymbol{\beta}_j, \boldsymbol{\gamma}_j, \boldsymbol{\omega}_j$	Model parameters used in simulation study ($\boldsymbol{\beta}_j \sim MN[\boldsymbol{\mu}_\beta, \boldsymbol{\Sigma}_\beta]$, $\boldsymbol{\gamma}_j \sim MN[\boldsymbol{\mu}_\gamma, \boldsymbol{\Sigma}_\gamma]$, $\boldsymbol{\omega}_j \sim MN[\boldsymbol{\mu}_\omega, \boldsymbol{\Sigma}_\omega]$), $j = 1,2, \ldots$
$\varepsilon_j(t)$	Noise term used in simulation study, $\varepsilon_j(t) \sim N(0, \sigma_\varepsilon)$, $j = 1,2, \ldots$
$\omega(\cdot)$	Proportion of time $t \in [0, T]$ that a curve belongs to a given band

References

Chang, S. I., and Yadama, S. 2010. "Statistical process control for monitoring non-linear profiles using wavelet filtering and B-spline approximation". *International Journal of Production Research*, 48(4), 1049-1068.

Cheng, C., Chiu, M. S. 2005. "Nonlinear process monitoring using JITL-PCA". *Chemometrics and Intelligent Laboratory Systems*, 76(1), 1-13.

Choi, S. W., Martin, E. B., Morris, A. J., and Lee, I. B. 2005. "Fault detection based on a maximum-likelihood principal component analysis (PCA) mixture". *Industrial & engineering chemistry research*, 44(7), 2316-2327.

Chou, S. H., Chang, S. I., and Tsai, T. R. 2014. "On monitoring of multiple non-linear profiles". *International Journal of Production Research*, 52(11), 3209-3224.

Chu, Y. H., Qin, S. J., and Han, C. 2004. "Fault detection and operation mode identification based on pattern classification with variable selection". *Industrial & engineering chemistry research*, 43(7), 1701-1710.

Colosimo, B.M., Pacella, M. 2007. "On the Use of Principal Component Analysis to Identify Systematic Patterns in Roundness Profiles", *Quality and Reliability Engineering International*, 23:6, 707 – 725

Colosimo, B.M., Pacella, M. 2010. "A Comparison Study of Control Charts for Statistical Monitoring of Functional Data", *International Journal of Production Research*, 48(6), 1575-1601

Cuevas A, Febrero M, Fraiman R. 2006. "On the use of bootstrap for estimating functions with functional data". *Computational Statistics and Data Analysis*, 51,1063–1074.

Cuevas, A., Febrero, M., Fraiman, R. 2007. "Robust estimation and classification for functional data via projection-based depth notions", *Computational Statistics*, 22, 481-496

Febrero, M., Galeano, P., and Gonzalez-Manteiga, W. 2008. "Outlier detection in functional data by depth measures with application to identify abnormal NOx levels". *Environmetrics* 19(4), 331-345.

Fraiman, R., Muniz, G. 2001. "Trimmed means for functional data", *Test*, 10(2), 419-440

Ge, Z., and Song, Z. 2008. "Online monitoring of nonlinear multiple mode processes based on adaptive local model approach". *Control Engineering Practice,* 16(12), 1427-1437.

Ge, Z., and Song, Z. 2009. "Multimode process monitoring based on Bayesian method". *Journal of Chemometrics,* 23(12), 636-650.

Ge, Z., Song, Z., and Gao, F. 2013. "Review of recent research on data-based process monitoring". *Industrial & Engineering Chemistry Research,* 52(10), 3543-3562.

Grasso, M., Colosimo, B. M., Semeraro, Q., Pacella, M. 2015. "A Comparison Study of Distribution-Free Multivariate SPC Methods for Multimode Data". *Quality and Reliability Engineering International,* 31(1), 75-96

Grasso, M., Menafoglio, A., Colosimo, B.M., Secchi P. 2016. "Using Curve Registration Information for Profile Monitoring", *Journal of Quality Technology*. 48(2), 99 - 127

Grasso, M., Colosimo, B. M., and Pacella, M. 2014. "Profile monitoring via sensor fusion: the use of PCA methods for multi-channel data". *International Journal of Production Research,* 52(20), 6110-6135.

Hastie, T., Tibshirani, R., Friedman, J. 2009. "The elements of statistical learning (Vol. 2, No. 1)". New York: Springer.

He, C., Girolami, M. 2004. "Novelty detection employing an L2 optimal non-parametric density estimator", *Pattern Recognition Letters,* 25, 1389-1397

He, F., Xu, J. 2016. "A novel process monitoring and fault detection approach based on statistics locality preserving projections". Journal of Process Control, 37, 46-57.

Hwang, D. H., and Han, C. 1999. "Real-time monitoring for a process with multiple operating modes". *Control Engineering Practice,* 7(7), 891-902.

Kang, L., and Albin, S. L. 2000. "On-Line Monitoring When the Process Yields a Linear Profile", *Journal of Quality Technology*, 32(4), 418-426

Jin, J., Shi, J. 2001. "Automatic Feature Extraction of Waveform Signals for In-process Diagnostic Performance Improvement", *Journal of Intelligent Manufacturing,* 12, 257 – 268

Lane, S., Martin, E. B., Kooijmans, R., and Morris, A. J. 2001. "Performance monitoring of a multi-product semi-batch process". *Journal of Process Control*, 11(1), 1-11.

Li, J., Cuesta-Albertos, J. A., and Liu, R. Y. 2012. "DD-classifier: Nonparametric classification procedure based on DD-plot". *Journal of the American Statistical Association*, 107(498), 737-753.

Lopes-Pintado, S., Romo, J. 2007. "Depth-based inference for functional data", *Computational Statistics & Data Analysis,* 51, 4957-4968

Lopes-Pintado, S., Romo, J., Torrente, A. 2010. "Robust depth-based tools for the analysis of gene expression data", *Biostatistics*, 11(2), 254-264

Markou, M., and Singh, S. 2003. "Novelty detection: a review—part 1: statistical approaches", *Signal processing*, 83(12), 2481-2497.

Noorossana R., Saghaei A., Amiri A. 2012. "Statistical Analysis of Profile Monitoring", *John Wiley & Sons*

Qiu, P., and Zou, C. 2010. "Control chart for monitoring nonparametric profiles with arbitrary design". *Statistica Sinica*, 20(4), 1655-1682.

Park, C., and Shrivastava, A. K. 2014. "Multimode Geometric-Profile Monitoring with Correlated Image Data and Its Application to Nanoparticle Self-Assembly Processes". *Journal of Quality Technology*, 46(3), 216-233

Ramsay, J. O. 2006. Functional data analysis, John Wiley & Sons, Inc.

Ren, S., Song, Z., Yang, M., Ren, J. 2015. "A novel multimode process monitoring method integrating LCGMM with modified LFDA". Chinese Journal of Chemical Engineering, 23(12), 1970-1980.

Sangalli, L. M., Secchi, P., Vantini, S., Vitelli, V., 2010. "K-mean alignment for curve clustering", *Computational Statistics & Data Analysis*, 54(5), 1219-1233

Srinivasan, R., Wang, C., Ho, W. K., and Lim, K. W. 2004. "Dynamic principal component analysis based methodology for clustering process states in agile chemical plants". *Industrial & engineering chemistry research*, 43(9), 2123-2139.

Tang, R., Müller, H. G. 2008. "Pairwise curve synchronization for functional data", *Biometrika*, 95(4), 875-889

Tukey, J. W. 1975. "Mathematics and the picturing of data". *Proceedings of the international congress of mathematicians*, 2, 523-531.

Wang, F., Tan, S., Peng, J., and Chang, Y. 2012. "Process monitoring based on mode identification for multimode process with transitions". *Chemometrics and Intelligent Laboratory Systems*, 110(1), 144-155.

Wasserman, L. 2006. "All of Nonparametric Statistics". *Springer Texts in Statistics*

Wen, Q., Ge, Z., & Song, Z. 2015. "Multimode Dynamic Process Monitoring Based on Mixture Canonical Variate Analysis Model". Industrial & Engineering Chemistry Research, 54(5), 1605-1614.

Woodall, W.H., Spitzner, D.J., Montgomery, D.C., Gupta, S. 2004. "Using Control Charts to Monitor Process and Product Quality Profiles", *Journal of Quality Technology*, 36(3), 309 - 320

Xie, X., and Shi, H. 2012. "Dynamic multimode process modeling and monitoring using adaptive Gaussian mixture models". *Industrial & Engineering Chemistry Research*, 51(15), 5497-5505.

Zhao, S. J., Zhang, J., and Xu, Y. M. 2004. "Monitoring of processes with multiple operating modes through multiple principal component analysis models". *Industrial & engineering chemistry research*, 43(22), 7025-7035.

Zhao, C., Yao, Y., Gao, F., and Wang, F. 2010. "Statistical analysis and online monitoring for multimode processes with between-mode transitions". *Chemical Engineering Science*, 65(22), 5961-5975.

Zhu, Z., Song, Z., and Palazoglu, A. 2012. "Process pattern construction and multimode monitoring". *Journal of Process Control*, 22(1), 247-262.

Zou, C., Qiu, P., and Hawkins, D. 2009. "Nonparametric control chart for monitoring profiles using change point formulation and adaptive smoothing"..*Statistica Sinica*, 19(3), 1337-1357.

Appendix A – PCA-based profile monitoring: a brief review of the method

Let $\mathbf{Y} = [\boldsymbol{Y}_1, \boldsymbol{Y}_2, \dots, \boldsymbol{Y}_J]^T$ be a the matrix of sampled profiles originated from the process in its current state, such that $\boldsymbol{Y}_j = [Y_{j,1}, Y_{j,2}, \dots, Y_{j,p}]^T$, $j = 1, \dots, J$. Let $\mathbf{Y}_{1:N}$ be an $N \times p$ matrix of $N < J$ in-control observations to be used to generate the reference PCA model (Phase I). The PCA consists of performing a spectral decomposition of the sample correlation matrix $\boldsymbol{S}_{1:M} = (1/(M-1))\, \mathbf{Y}_{1:N}^T \mathbf{Y}_{1:N}$, i.e. finding the matrices $\mathbf{L}$ and $\mathbf{U}$ that satisfy the relationship:

$$\mathbf{U}^T \mathbf{S}_{1:N} \mathbf{U} = \mathbf{L} \tag{B1}$$

where $\mathbf{L}$ is a diagonal matrix whose diagonal elements are the eigenvalues of $\mathbf{S}_{1:M}$ (λ_i; $i = 1, \dots, p$), while $\mathbf{U}$ is an orthonormal matrix whose i^{th} column $\mathbf{u}_i$ is the i^{th} eigenvector of $\mathbf{S}_{1:N}$.

The projection of the j^{th} sample onto the K-dimensional Principal Component (PC) orthogonal space is defined as follows:

$$\mathbf{z}_j = \mathbf{U}^T(\boldsymbol{Y}_j - \overline{\boldsymbol{Y}}) = \left[z_{j,1}, \dots, z_{j,K}\right]^T \qquad (j = 1,2, \dots, J) \tag{B2}$$

where $\overline{\boldsymbol{Y}} = (1/N)\sum_{j=1}^{N} \boldsymbol{Y}_j$ is the average profile among the N ones used to estimate the PCA model. K is the maximum number of PCs that can be extracted, i.e. the maximum number of non-zero eigenvalues. K is upper-bounded by $\min\{p, N\}$.

The relative importance of each PC, i.e. the amount of explained variance, is represented by the value of the corresponding eigenvalue. Therefore, the relevant information content may be captured by a reduced number of PCs, providing the dimensionality reduction at the origin of the PCA popularity. A commonly used approach consists of setting a threshold on the amount of variance explained by each PC and retain the minimum number of PCs that capture that amount. By retaining the first m PCs, each sample – i.e. each row of the data matrix may be reconstructed as follows:

$$\widehat{\boldsymbol{Y}}_j(m) = \overline{\boldsymbol{Y}} + \sum_{i=1}^{m} z_{j,i}\mathbf{u}_i \qquad (j = 1,2,\dots,J) \tag{B3}$$

The process monitoring strategy requires the computation of two statistics (Colosimo and Pacella, 2007): one is the Hotelling's T^2 statistics, used to detect possible deviations along the directions of the first m PCs:

$$T_j^2(m) = \sum_{i=1}^{m} \frac{z_{j,i}^2}{\lambda_i} \qquad (j = 1,2,\dots,J) \tag{B4}$$

The second is the Sum of Prediction Errors (SPE) statistics, used to detect possible deviations in directions orthogonal to the ones associated to the first m PCs, given by:

$$SPE_j(m) = (\widehat{\boldsymbol{Y}}_j(m) - \overline{\boldsymbol{Y}})^T(\widehat{\boldsymbol{Y}}_j(m) - \overline{\boldsymbol{Y}}) \qquad (j = 1,2,\dots,J) \tag{B5}$$

The theoretical Phase II control limit used for T^2 chart is:

$$UCL_{T^2} = cF_\alpha(m, N-m) \tag{B6}$$

where α is the type I error, whereas $F_\alpha(m, N-m)$ is the $(1-\alpha)\%$ percentile of the Fisher distribution with degrees of freedom m and $N-m$, respectively, and c is given by:

$$c = [m(N+1)(N-1)/N(N-m)] \quad \text{(B7)}$$

Regarding the SPE control chart, one possible control limit formulation proposed is based on the observation that the following quantity is approximately normally distributed with zero mean and unit variance:

$$c = \frac{\theta_1[(Q/\theta_1)^{h_0} - 1 - \theta_2 h_0(h_0-1)/\theta_1^2]}{\sqrt{2\theta_2 h_0^2}} \quad \text{(B8)}$$

where $\theta_i = \sum_{j=m+1}^{P} L_{j,j}^i$, with $i = 1,2,3$, and $h_0 = 1 - (2\theta_1\theta_3)/3\theta_2^2$. Then, the theoretical control limit for the SPE control chart is:

$$UCL_{SPE} = \theta_1 \left[\frac{c(\alpha)\sqrt{2\theta_2 h_0^2}}{\theta_1} + 1 + \frac{\theta_2 h_0(h_0-1)}{\theta_1^2} \right]^{\frac{1}{h_0}} \quad \text{(B9)}$$

where $c(\alpha)$ is the $(1-\alpha)\%$ percentile of the normal distribution.

Eventually, the Bonferroni's rule for independent events is used to design the control limits. In case of departures from the normality assumption of monitored data, empirical control limits can be estimated via kernel density estimation of the control statistics distributions under IC conditions.

Appendix B – Alternative functional data depth formulations

The FMD represents a simple generalization of the data depth concept to the FDA framework. It consists of computing the univariate depth at any given time point $t \in$

$[0, T]$ and then integrating the local depth measures over the interval $[0, T] \subset \mathbb{R}$ (see Fraiman and Muniz (2001) for further details). The MBD (Lopes-Pintado and Romo, 2007) is, instead, a graph based depth measure, where the term "*graph*" of a function $Y_j(t): t \in [0, T]\}$ denotes the subset of the plane $G\left(Y_j(t)\right) = \left\{\left(t, Y_j(t)\right): t \in [0, T]\right\}$.

A band in $\mathbb{R}^2$ delimited by a set of n curves $X_1(t), X_2(t), \ldots, X_n(t)$ is defined as follows:

$$B\big(X_1(t), \ldots, X_n(t)\big) = \left\{(t, Y): t \in [0, T], \min_{k=1,\ldots,n} X_k(t) \leq Y \leq \max_{k=1,\ldots,n} X_k(t)\right\} \qquad \text{(A1)}$$

The quantity:

$$S_{n,q}\left(Y_j(t)\right) = \binom{n}{q}^{-1} \sum_{1 \leq i_1 \leq \cdots \leq i_q \leq n} \omega\left\{G\left(Y_j(t)\right) \subset B\big(X_1(t), \ldots, X_n(t)\big)\right\} \qquad \text{(A2)}$$

where $q \geq 2$, expresses the proportion of bands $B\big(X_1(t), \ldots, X_n(t)\big)$ determined by q different curves containing the graph of $Y_j(t)$, where $\omega(\cdot)$ is the proportion of time $t \in [0, T]$ that $Y_j(t)$ is included into the band. Then, the MBD of $Y_j(t)$ can be computed as follows:

$$D_j(n, Q) = \sum_{q=2}^{Q} S_{n,q}\left(Y_j(t)\right), \qquad Q \geq 2, \qquad j = 1,2, \ldots \qquad \text{(A3)}$$

Where Q is a tuning parameter. Lopez-Pintado and Romo (2007) showed that the depth measure is robust with respect to the choice of Q, and the use of any value $Q \geq 2$ does not change the ranking among curves.

Table 1 - Cutting parameters corresponding to different end-milling modes (the spindle speed was always 253 rpm)

Cut order	Mode	A_z - Feed rate (mm/z)	D_r - Radial depth of cut (mm)	D_a - Axial depth of cut (mm)	Tool copy
1	A	0.2	40	8	1
2	B	0.2	40	8	2

Table 2 – Mean vector $\boldsymbol{\mu}_{\omega}$ used to generate different profile patterns in different modes

	Mode	$\boldsymbol{\mu}_{\omega}$
Historical IC modes (database)	A	$[-0.50, -0.45, -0.30, 0.70, -0.45]$
	B	$[-0.50, -0.20, -0.30, 0.70, -0.45]$
	C	$[-0.50, -0.45, -0.55, 0.70, -0.45]$
	D	$[-0.50, -0.45, -0.30, 0.70, -0.20]$
New modes	E	$[-0.50, -0.75, -0.30, 0.70, -0.45]$
	F	$[-0.50, -0.45, -0.10, 0.70, -0.45]$
	G	$[-0.50, -0.45, -0.30, 0.70, -0.75]$
	H	$[-0.30, -0.45, -0.30, 0.70, -0.45]$

Table 3 - Model parameters for multimode pattern generation in Scenario 2

Mode	μ_i	σ_i
A	{25 35 40 45 60 100 150 180}	{6 3 4 2 3 20 10 3}
B	{25 35 40 45 60 100 150 180}	{9 6 7 5 3 20 10 3}
C	{25 35 40 45 60 100 150 180}	{6 3 4 2 3 25 15 8}
D	{25 35 40 45 60 100 150 180}	{8 5 6 4 5 22 12 5}
E	{25 30 40 45 65 100 150 180}	{6 3 4 2 3 20 10 3}
F	{25 35 40 45 60 90 160 180}	{6 3 4 2 3 20 10 3}
G	{25 35 40 45 60 100 145 185}	{6 3 4 2 3 20 12.5 5.5}
H	{25 40 40 50 60 100 150 180}	{6 8 4 7 3 20 10 3}

Table 4 - 95% confidence intervals of type I errors in Scenario 1 and Scenario 2

	Modes in design phase	Mode in testing phase (Scenario 1)							
		A		B		C		D	
1	A,B,C,D	(0.013	0.017)	(0.007	0.009)	(0.012	0.015)	(0.007	0.009)
2	A	**(0,010**	**0,011)**	(0,106	0,116)	(0,096	0,108)	(0,095	0,106)
	B	(0,091	0,103)	**(0,010**	**0,011)**	(0,095	0,107)	(0,089	0,101)
	C	(0,097	0,108)	(0,096	0,107)	**(0,009**	**0,012)**	(0,091	0,103)
	D	(0,092	0,105)	(0,089	0,101)	(0,090	0,100)	**(0,008**	**0,010)**
	Modes in design phase	Mode in testing phase (Scenario 2)							
		A		B		C		D	
1	A,B,C,D	(0,019	0,024)	(0,001	0,003)	**(0,007**	**0,010)**	(0,011	0,014)
2	A	**(0,010**	**0,011)**	(0,096	0,107)	(0,102	0,112)	(0,093	0,103)
	B	(0,090	0,101)	**(0,009**	**0,012)**	(0,091	0,102)	(0,100	0,113)
	C	(0,091	0,102)	(0,091	0,101)	**(0,010**	**0,011)**	(0,094	0,107)
	D	(0,094	0,107)	(0,101	0,113)	(0,095	0,106)	**(0,010**	**0,010)**

Figure captions

Fig. 1 – Scheme of the basic multi-modelling approach (a) and scheme of the generalized multi-modelling method proposed in this study (b)

Fig. 2 – Experimental set-up for cutting force signal acquisition in end-milling on a Ti-6Al-4V part

Fig. 3 – IC cutting force profile patterns (grey) acquired in end-milling cut 1 (a.k.a. Mode A) (left panel) and cut 2 (a.k.a. Mode B) (right panel); each profile consists of $p = 264$ data-points; cross-section average profiles are depicted with black thick lines

Fig. 4 – Superimposition of Mode A profile data (solid grey curves) and the first three curves in cut 2 (Mode B) (red-dashed, blue-dotted and green-dot-dashed curves); the black thick line represents the cross-section average profile in Mode A

Fig. 5 – T^2 and SPE control charts for the proposed approach; the vertical solid line separates the design phase (on the left) from the use phase (on the right)

Fig. 6 – Cutting force profile patterns (grey) acquired in cut 3; each profile consists of $p = 264$ data-points; cross-section average profiles are depicted with black thick lines

Fig. 7 – T^2 and SPE control charts for the traditional approach; the vertical solid line separates the design phase (on the left) from the use phase (on the right)

Fig. 8 – Simulated profile patterns in different modes (Scenario 1): 100 profile realizations in each mode (grey curves) and cross-section average profiles (black thick lines)

Fig. 9 – 95% confidence intervals of misclassification errors in Scenario 1 for the proposed approach (MD) and competitor methods ($J = 50, M = 1$)

Fig. 10 – 95% confidence intervals of novelty detection errors in Scenario 1 for the proposed approach (MD) and competitor methods ($J = 50, M = 1$)

Fig. 11 – Misclassification error in mode A, Scenario 1 (left panel) and novelty detection error in mode E, Scenario 1 (right panel) for the MD-based approach and the KNN-based approach, for different values of parameter M ($J = 50$)

Fig. 12 – Simulated profile patterns in different modes (Scenario 2): 100 profile realizations in each mode (grey curves) and cross-section average profiles (black thick lines)

Fig. 13 – 95% confidence intervals of misclassification errors in Scenario 2 for the proposed approach (MD) and competitor methods ($J = 50, M = 1$)

Fig. 14 – 95% confidence intervals of novelty detection errors in Scenario 2 for the proposed approach (MD) and competitor methods ($J = 50, M = 1$)